

## Mobility of DR1 Molecules Embedded in Nanostructured PMMA Films

J. A. García-Macedo<sup>a</sup>, A. Franco, G. Valverde-Aguilar, M. A. Ríos-Enríquez

Departamento de Estado Sólido, Instituto de Física, Universidad Nacional Autónoma de México,  
México, D. F. C. P. 04510. Fax: +52(55) 56 22 50 00; Telephone: +52(55) 56 22 51 03

<sup>a</sup>gamaj@fisica.unam.mx (corresponding author)

Received: July 15<sup>th</sup>, 2007, revised: January 12<sup>th</sup>, 2008, accepted: February 23<sup>rd</sup>, 2008

**Keywords:** polymers, nanostructure, second harmonic generation, Corona poling.

**Abstract.** The kinetics of the orientation of Disperse Red 1 (DR1) molecules embedded in nanostructured Polymethylmetacrylate (PMMA) films was studied under the effect of an intense constant electric poling field. The changes in the orientation distribution of the DR1 molecules were followed by Second Harmonic Generation (SHG) measurements. The SHG signal was recorded as function of time at three different temperatures. We focused on both, the signal increases under the presence of the poling field and the signal decays without the poling field. The studied PMMA films were nanostructured by the incorporation of ionic surfactants as the Sodium Dodecyl Sulfate (SDS) and the Cetyl Trimethyl Ammonium Bromide (CTAB) during their preparation. The kinds of nanostructures obtained in the films were determined by means of X-ray diffraction (XRD) measurements. Substantial differences in signal intensity and in growth and decay rates between amorphous and nanostructured films were found.

### Introduction

It is possible to induce non-centrosymmetric order in some materials by means of the application of a strong electric field at appropriate temperatures. For example, this process can be carried out with the procedure known as Corona poling [1,2]. In a chromophores-containing polymeric film, the non-centrosymmetric order implies a nanoscale order of the permanent dipolar moment of chromophores along a preferential direction. This phenomenon is attractive for second order nonlinear optical applications [3-5]. In fact, by means of the SHG, it is possible to follow in situ the orientation of the chromophores embedded in the polymer [6,7]. As the orientation of the chromophores is highly dependent of their surrounding medium, it is useful to know the local environment around the chromophores. A good way to know the effect of local environment over the chromophores is to studying their orientational kinetics [8,9]. We expect that different nanostructures in the polymeric host generate different local environments around the chromophore, which should be reflected in SHG signal measurements as function of poling time. In fact, there is a recent interest in studying the optical properties of orientable chromophores immersed in self-assembled nanostructured media [10].

In this paper we present SHG dynamics results for nanostructured PMMA films containing DR1 chromophores. In this work we define a nanostructured material to that one whose matrix has a periodic long-range order. Two different long-range nanophases were detected on these films by XRD measurements. These nanophases were: (1) a lamellar phase and (2) a mixture of lamellar and hexagonal phases.

The chromophores orientation dynamics has also been theoretically studied by J. W. Wu [11] and D. J. Binks *et al.* [12] who have proposed models for the description of this phenomenon based on a rotational diffusion equation. But to analyze the experimental results we preferred to use a model developed by us [13,14], which is a phenomenological one based on the harmonic movement of the chromophores embedded inside the films.

The knowledge of the temporal behavior of the SHG signal in these kinds of materials can give information about the local interactions between the chromophores and their surrounding medium, which is very important for the optimal development of nanophotonic devices.

## Materials Synthesis

All the reactants were of laboratory reagent grade (Aldrich) and used as received. DR1 was the photoactive chromophore in all the samples. All the samples were guest-host, and the DR1 concentration was the same for all the PMMA samples.

The PMMA amorphous samples were prepared as follows: PMMA (F.W.=120,000 g·mol<sup>-1</sup>) and Tetrahydrofuran (THF) were mixed and stirred for 15 minutes at room temperature. Then DR1 was added and the mixture was stirred for another 15 minutes. This final solution was filtered with a 0.45 μm pore size syringe filter. 80% of the total weight was liquid (THF), and 20% was solid (PMMA+DR1). 95% of the solid weight was PMMA and 5% was DR1. The films were deposited onto microscopic glass slides by dip-coating at a constant withdrawal speed of 20 cm/min, and annealed at 80°C during 4 hours without controlled atmosphere.

The PMMA nanostructured samples were prepared in a similar procedure, but the ionic surfactant was added just prior to filter, and the final solution was stirred for 5 minutes. In this case, the surfactants remained inside the material as the annealing temperature was low.

Three different kinds of the matrix organization were identified from the XRD patterns: amorphous, lamellar and mixed nanostructures. The mixed phase was obtained by adding 1.5 wt % of the cationic surfactant CTAB during the PMMA matrix formation process in liquid phase. The long-range order lamellar nanostructure was obtained by the incorporation of 1.5 wt % of the anionic surfactant SDS during the PMMA matrix formation process the liquid phase. XRD patterns were recorded on a Bruker AXS D8 Advance diffractometer using Ni-filtered CuKα radiation. A step-scanning mode with a step of 0.02° in the range from 1.5° to 10° in 2θ and an integration time of 2 s were used.

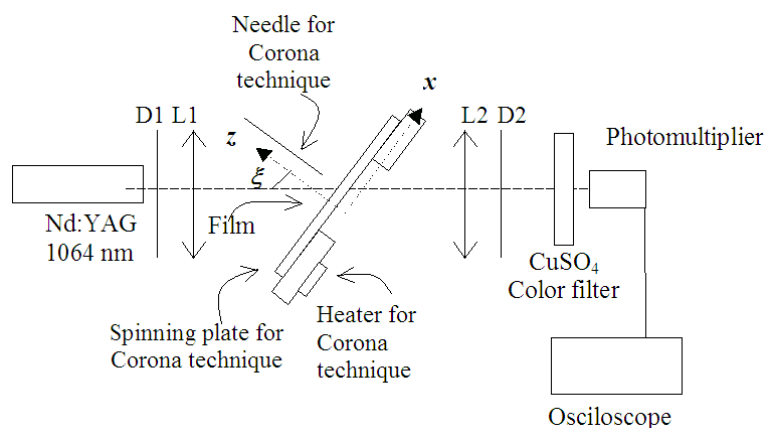


**Figure 1.** Schematic diagram of the SHG experimental setup. The coordinate system is such that the copper plate is on the  $x$ - $y$  plane, and the corona field along the  $z$ -axis. The angle between the  $z$ -axis and the fundamental beam of light is  $\xi$ .

The SHG measurements were carried out in situ by using the experimental set-up shown in Fig. 1. This set-up consists of a pulsed YAG:Nd (Nanolase NP-10620-100, wavelength: 1064 nm, frequency: 5 kHz, energy: 5 μJ/pulse) laser as fundamental light source, two lenses, one of them focus the fundamental laser beam on the sample; the second one, which is at the back of the sample at the focal distance from the sample, collects the light generated by the sample and sends it to a photomultiplier (Hamamatsu H5784) through a color filter which blocks the fundamental excitation. The photomultiplier was connected to an oscilloscope (Tektronix TDS 3052B) and the data were stored by a computer each 0.5 seconds. For the SHG measurements, the films were supported on a copper plate which has a home-made temperature controller and a hole through which the fundamental and the harmonic beams of light pass. Corona field was produced by applying a high voltage (~5 KV) between the needle and the plate (distance from the copper plate: 1.2 cm).

## Results and Discussion

**XRD patterns.** The XRD patterns obtained for the samples templated with SDS and CTAB are shown in the Fig. 2. The XRD pattern for the sample with SDS (Fig. 2, left) corresponds to a lamellar nanostructure (the peaks follow the  $1q^*$ ,  $2q^*$ ,  $3q^*$ ,... sequence [15,16]) with a  $d$ -spacing equal to 3.8 nm and  $q^*=2\pi/d$ . The corresponding XRD pattern for the sample with CTAB (Fig. 2, right) reveals the coexistence of two phases, a lamellar and a hexagonal nanostructure (the hexagonal nanostructure with a  $1q^*$ ,  $(3)^{1/2}q^*$ ,... sequence [15,16], where  $q^*=4\pi/d(3)^{1/2}$ ). The lamellar phase had a  $d$ -spacing equal to 3.8 nm and the hexagonal phase had a  $d$ -spacing equal to 5.2 nm.

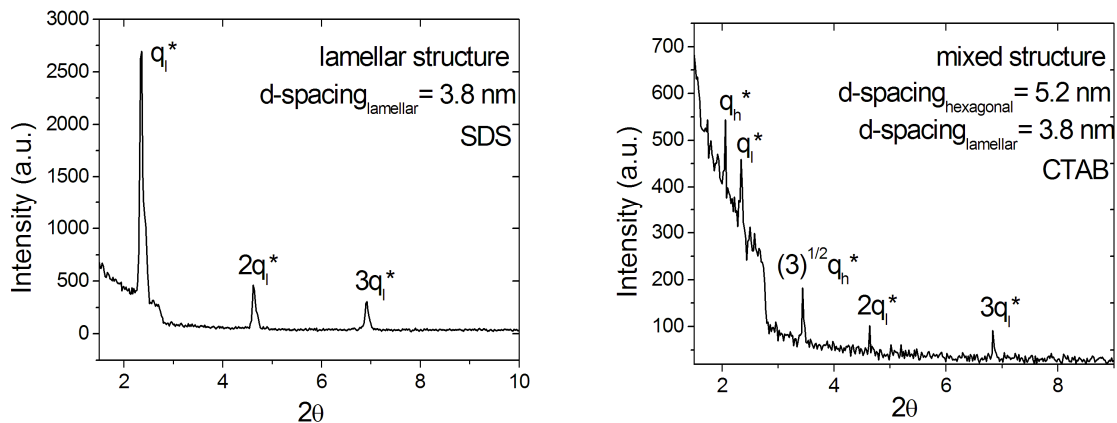


**Figure 2.** XRD patterns at low angle of the samples templated with SDS (left) showing a lamellar nanostructure, and CTAB (right) showing a mixed nanostructure.

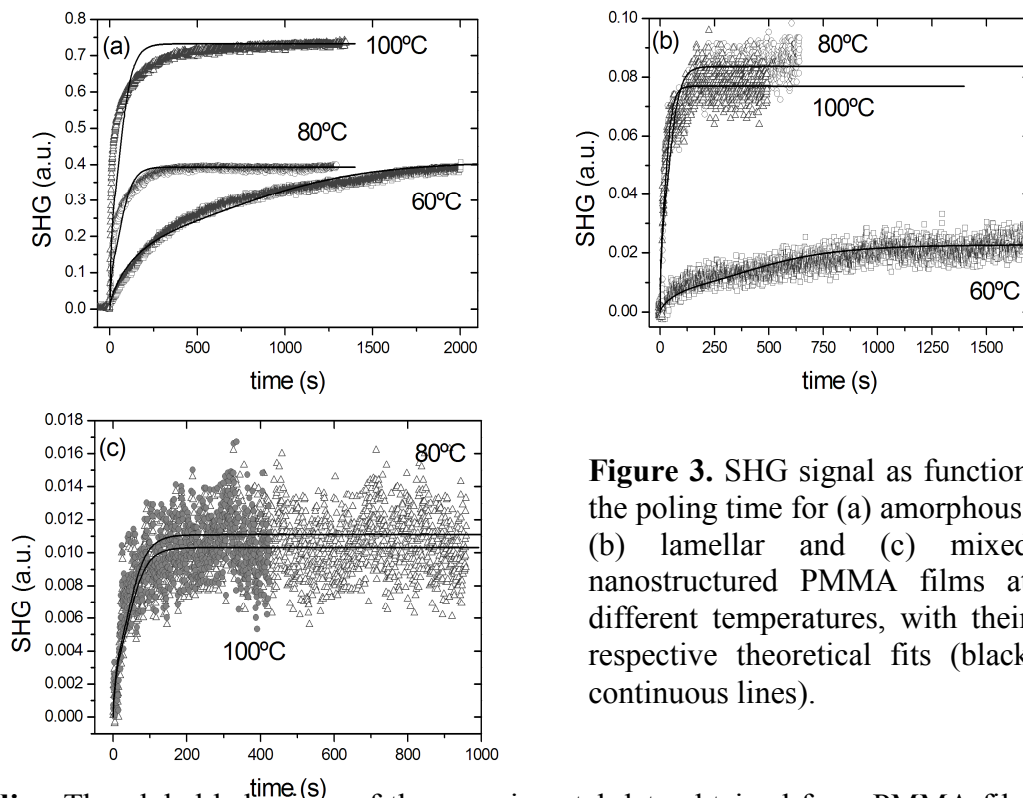


**Figure 3.** SHG signal as function the poling time for (a) amorphous, (b) lamellar and (c) mixed nanostructured PMMA films at different temperatures, with their respective theoretical fits (black continuous lines).

**SHG studies.** The global behaviour of the experimental data obtained from PMMA films consists in a growth of the SHG signal as the poling time increases, until the signal reaches a plateau at enough large poling times. The variations of the SHG signal intensities as the function of poling

time are shown in Fig. 3 for different temperatures. Fig. 4 shows the SHG intensity as function of the poling time for each nanophase at 60°C, 80°C and 100°C. In fact, Fig. 3 and Fig. 4 have the same experimental data but rearranged in different way for the sake of clarity.

The experimental data were fitted using a chromophores orientation model previously reported by us [13], which requires two fitting parameters: (1) a damping constant of the material ( $\gamma$ ), directly related to the chromophore-matrix interactions and inversely proportional to the mobility, and (2) a SHG intensity signal constant ( $C$ ), proportional to  $(N\beta_{333}I^{\omega})^2$ , where  $N$  is the number of non-linear optical active chromophores (DR1 in our case),  $\beta_{333}$  the second order hyperpolarizability of the chromophores and  $I^{\omega}$  the intensity of the fundamental beam of light. Thus, larger  $\gamma$  values imply lower chromophore mobilities, and larger  $C$  values imply larger number of molecules contributing to the non-centrosymmetry of the material. Besides, the model requires an experimental determination of the second order parameter ( $A_2$ ) maximum value through the equation:

$$A_2 = 1 - \frac{A_{\perp}}{A(t=0)} \quad (1),$$

where  $A_{\perp}$  is the optical absorbance of the film at the resonance chromophore peak after a very large poling time and  $A(t=0)$  is the optical absorbance of the film at the resonance chromophore peak before the poling procedure. This value is directly related to the percentage of orientable chromophores in the material, and this value also allows to calculate the local electric field inside the film ( $E$ ) [13], without chromophore-chromophore interaction corrections.

Basically, the chromophore kinetic is described by a harmonic oscillator equation:

$$\ddot{\theta} + 2\gamma\dot{\theta} + \omega^2\theta = 0 \quad (2),$$

where ( $\omega$ ) is the natural frequency of the chromophores, which have a dipolar moment ( $\mu_3$ ) and an inertia moment ( $I_{33}$ ). These parameters are related by the next equation:

$$\omega = \sqrt{\frac{\mu_3 E}{I_{33}}} \quad (3).$$

Besides, the electric field ( $E$ ) is calculated from the maximum order parameter determined by means of the next Rigid Oriented Gas Model equation [1]:

$$A_2(u) = 1 + \frac{3}{u^2} - \frac{3}{u} \coth(u) \quad (4)$$

with ( $u$ ) the electrostatic and thermal energies ratio, where

$$u = \frac{\mu_3 E}{k_b T} \quad (5).$$

Table 1 contains the parameters used to fit the experimental data from Figs. 3 and 4. In this table, the  $D$  parameter is also included.  $D$  was used to fit the experimental data from the Fig. 5. These experimental data correspond to the SHG signal intensity decay after turning off the poling field under a constant temperature. The fits of Fig. 5 were obtained by using a single exponential curve:

$$Y = Y_0 + Y_1 e^{-Dt} \quad (6),$$

where  $Y_0$  is a baseline value (which is constant, and does not have information about the chromophores kinetics),  $(Y_1+Y_0)$  is the SHG intensity signal before relaxing the chromophores orientation, and  $D$  contains the information of the mobility of the chromophores in the films (as  $\gamma$  do in the signal growth case).

**Table 1.** Parameters of the best fitting to the experimental results obtained for each studied film.  $\gamma$ ,  $C$  and  $D$  are fitting parameters.  $A_2$  was obtained experimentally and  $E$  is a fitting consequence.

Sample	$A_2$ (maximum)	$\gamma$ ( $\cdot s^{-1}$ ) $\times 10^{24}$	$C$ (a.u.)	$D$ ( $s^{-1}$ ) $\times 10^{-3}$	$E$ ( $V m^{-1}$ ) $\times 10^8$
PMMA Amorphous 60°C	0.36	13.000	3.76	2.82	5.23
PMMA Amorphous 80°C	0.05	0.261	6.94	21.92	1.52
PMMA Amorphous 100°C	0.19	0.639	2.07	14.83	3.60
PMMA SDS 60°C	0.10	2.221	0.5	10.67	2.12
PMMA SDS 80°C	0.16	0.360	1.1	58.00	2.99
PMMA SDS 100°C	0.16	0.240	1.0	98.33	3.16
PMMA CTAB 60°C	-----	-----	-----	-----	-----
PMMA CTAB 80°C	0.02	0.120	0.09	68.33	1.04
PMMA CTAB 100°C	0.08	0.240	0.04	68.33	2.06

With respect to  $A_2$ , it is important to mention that the obtained values are the maximum ones. These values do not correspond to chromophore degradation because the SHG signal was followed during several identical poling cycles and in all the cases the SHG signal reached the same maximum value.

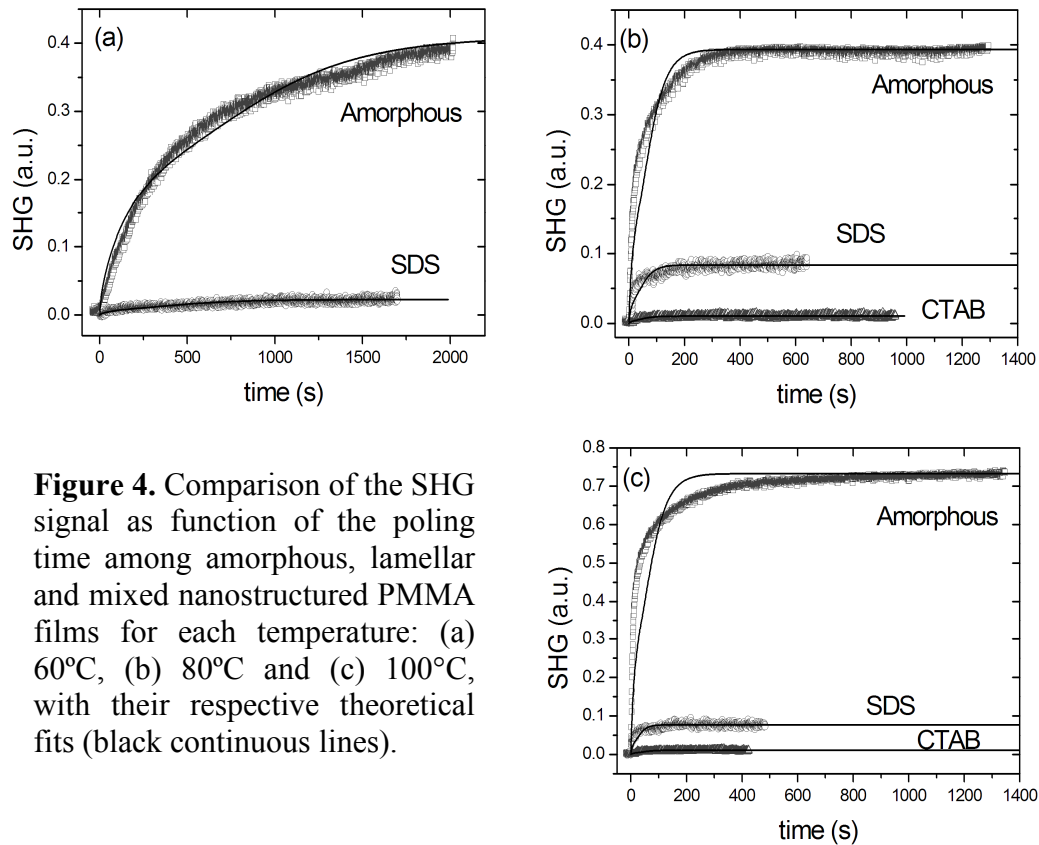


**Figure 4.** Comparison of the SHG signal as function of the poling time among amorphous, lamellar and mixed nanostructured PMMA films for each temperature: (a) 60°C, (b) 80°C and (c) 100°C, with their respective theoretical fits (black continuous lines).

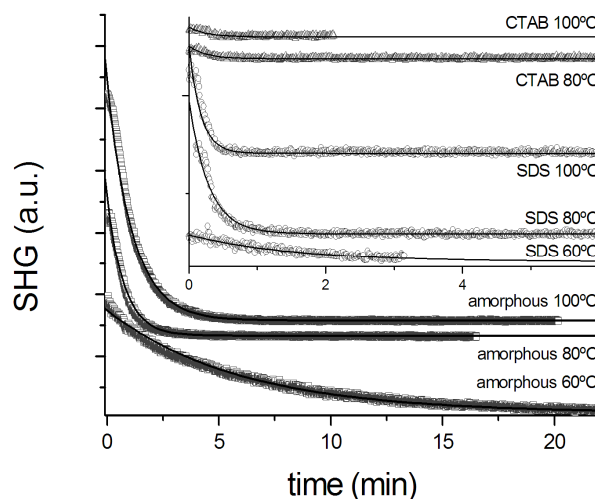
It is possible to see from Table 1 that the changes in the chromophore mobility inside the films are consistent between the growth ( $\gamma$ ) and the decay ( $D$ ) processes of the SHG signal. Generally, the chromophore mobility increases ( $\gamma$  decreases) when the temperature increases, but the amorphous films exhibited a maximum mobility at 80°C. In this sense, the surfactants give more stability to the films. In the case of the films with CTAB (those with mixed nanostructure) we were not able to detect any SHG signal at 60°C, that means the chromophores did not have enough mobility at that temperature. It was only after increasing the temperature at 80°C that there was chromophores orientation under the application of the corona field, and we observed practically the same mobility values at 80°C than at 100°C.

As can be seen from Fig. 4, the fits of the nanostructured samples were better than the fits corresponding to the amorphous films. We argue that the amorphous PMMA matrix also experiences some changes under the application of a corona field (which were detected by the SHG system), otherwise there should be a permanent distribution of several  $\gamma$  values in the films. All the fits in Fig. 5 clearly show a good agreement between the SHG signal decay and a single-exponential behaviour, which is representative of a pure diffusion process governed by single  $\gamma$  value (as a matter of fact,  $D$  is related to the diffusion constant of the system).

From Table 1, the  $A_2$  order parameter values reflect the anomalous behaviour of the amorphous PMMA films at 80°C. While the order parameter values increased with the increase of temperature for the nanostructured films, the  $A_2$  values decreased with temperature for the amorphous PMMA films, furthermore there is a minimum value at 80°C. The  $A_2$  parameter is a measurement of the amount of orientable chromophores in the films and is directly related to the electric field inside the film ( $E$ ) under the presence of the poling field, thus large  $A_2$  values imply large number of orientable molecules or a large magnitude of the electric field ( $E$ ). If we consider a set of films with the same kind of matrix and the same chromophores concentration, then the unique variable is the poling temperature. On the other hand, if we assume no change in the matrix of the films under the Corona procedure, then the changes in  $A_2$  should be due to the changes in the effective number of orientable chromophores in the material. Thus, as the temperature increases

there are more effective orientable chromophores in the nanostructured films. However, in the amorphous films there should be some changes in the matrix as the temperature increases, as no increment in the orientable chromophores was detected. Possibly, the glass transition temperature of the film plays an important role on such behaviour, which at this moment we could not determine precisely.

**Figure 5.** SHG decay signal for all the PMMA films at 60°C, 80°C and 100°C. Experimental data were fitted with an exponential decay (black continuous line).



Besides, the  $C$  values (Table 1) give information about how many chromophores could be oriented non-centrosymmetrically, assuming that the chromophores were not degraded under the Corona field (i.e. assuming  $\beta_{333}$  is constant). The  $C$  value of the films increases with the increase of temperature, and has a maximum at 80°C. The largest values were obtained for the amorphous films and the lowest values for the films with CTAB. From 80°C to 100°C the  $C$  value decreases and the lowest value was obtained for the films with SDS. Again, 80°C seems to be a critical temperature for the PMMA films, nevertheless the presence of the surfactants diminishes its consequences, in the sense that the surfactants give stability to the films.

In summary, when we compare the nanostructured PMMA films with the amorphous PMMA films, the first ones showed increased chromophores mobility, decreased number of orientable chromophores and better stability at higher temperatures. Apparently, the mobility depends on how much the surfactants tailored the arrangement of the matrix.

At 80°C and 100°C, the lowest value of the  $A_2$  parameter was obtained for the PMMA films containing CTAB. At 80°C the highest  $A_2$  value was obtained for the PMMA films containing SDS, while at 100°C the highest value was observed for the amorphous PMMA films. At 80°C and 100°C, the highest value of the  $C$  parameter was obtained for the amorphous PMMA films, and the lowest value was obtained by the PMMA films containing CTAB. It means that the amorphous PMMA films experience some structural change at 80°C. In general, the amorphous PMMA films have the largest number of non-centrosymmetrically orientable molecules and the PMMA film containing CTAB have the lowest number.

Thus, the surfactants increase the chromophores mobility but decrease the number of orientable chromophores. These features depend of the kind of surfactant used in the films synthesis.

## Conclusions

High optical quality amorphous and nanostructured PMMA films doped with the chromophore DR1 were synthesized. A long-range ordered nanostructure was obtained in the PMMA films.

Second harmonic generation experimental results as a function of the poling time in PMMA:DR1 guest-host films were successfully fitted with a physical model [13]. This macroscopic response depends on the orientation and interaction of these nanoscopic molecules.

The SHG signal intensity was identified with the number of non-centrosymmetrically orientable chromophores. The rise and decay times of the SHG signal were identified with the mobility of the orientable chromophores.

The largest maximum SHG signal was measured for the amorphous PMMA films, and the lowest for PMMA films with mixed nanostructure. The SHG signal intensity varied in the sequence: Amorphous PMMA > SDS PMMA > CTAB PMMA. Besides, among the PMMA films the shortest rise time for the SHG signal was observed in the films with mixed nanostructure, and the largest one was obtained in the amorphous films. The shortest decay time for the SHG signal was observed in the films with mixed nanostructure, and the longest was observed in the amorphous PMMA films. The SHG signals grew with temperature and reached saturation faster at high temperature.

## Acknowledgements

CONACyT 89584, CONACyT 79781, NSF-CONACyT, PUNTA, PAPIIT 116506-3 and ICyTDF supported this work. The authors also thank to Sci. M. in Sci. Manuel Aguilar-Franco (XRD) for technical assistance. GVA thanks to ICyTDF for postdoctoral fellowship. We thank to Carlos Aguilar-Gutiérrez for his help to take SHG measurements.

## References

- [1] M. A. Mortazavi, A. Knoesen, and S. T. Kowel, B. G. Higgings, A. Dienes: *J. Opt. Soc. Am. B* Vol. 6 (1989), p. 733
- [2] J. A. Giacometti, S. Fedosov, and M. M. Costa: *Braz. J. Phys.* Vol. 29 (1999), p. 269
- [3] G. Della Giustina, G. Brusatin, M. Guglielmi, M. Dispenza, A. M. Fiorello, M. Varasi, M. Casalboni, A. Quatela, F. De Matteis, E. Giorgetti, G. Margheri, P. Innocenzi, A. Abbotto, L. Beverina, and G. A. Pagani: *Mat. Sci. & Eng. C* Vol. 26 (2006), p. 979
- [4] W. Shi, C. S. Fang, Q. W. Pan, Z. H. Qin, Q. T. Gu, D. Xu, and J. Z. Yu: *J. Phys. D App. Phys.* Vol. 35 (2002), p. 1404
- [5] F. Chaput, D. Riehl, J. P. Boilot, K. Cargnelli, M. Canva, Y. Lévy, and A. Brun: *Chem. Mater.* Vol. 8 (1996), p. 312
- [6] A. W. Harper, S. Sun, L. R. Dalton, S. M. Garner, A. Chen, S. Kalluri, W. H. Steier, and B. H. Robinson: *J. Opt. Soc. Am. B* Vol. 15 (1998), p. 329
- [7] M. Eich, A. Sen, H. Looser, G. C. Bjorklund, J. D. Swalen, R. Twieg, and D. Y. Yoon: *J. Appl. Phys.* Vol. 66 (1989), p. 2559
- [8] T. Goodson III and C. H. Wang: *J. Phys. Chem.* Vol. 100 (1996), p. 13920
- [9] I. G. Marino, D. Bersani, and P. P. Lottici: *Opt. Mat.* Vol. 15 (2000), p. 175
- [10] Y. Tian, Ch.-Y. Chen, M. A. Haller, N. M. Tucker, J. -W. Ka, J. Luo, S. Huang, and A. K.-Y. Jen: *Macromolecules* Vol. 40 (2007), p. 97
- [11] J. W. Wu: *J. Opt. Soc. Am. B* Vol. 8 (1991), p. 142
- [12] D. J. Binks, K. Khand, and D. P. West: *J. Appl. Phys.* Vol. 89 (2001), p. 231
- [13] A. Franco, G. Valverde-Aguilar, J. García-Macedo, M. Canva, F. Chaput, and Y. Levy: *Optical Materials* Vol. 29 (2006), p. 6
- [14] A. Franco, G. Valverde-Aguilar, and J. García-Macedo: *Optical Materials* Vol. 29 (2007), p. 814
- [15] J. Merta, M. Torkkeli, T. Ikonen, R. Serimaa, and P. Stenius: *Macromolecules* Vol. 34 (2001), p. 2937
- [16] P. Alexandridis, U. Olsson, and Björn Lindman: *Langmuir* Vol. 14 (1998), p. 2627

---

**Journal of Nano Research Vol. 5**

doi:10.4028/0-00000-029-9

**Mobility of DR1 Molecules Embedded in Nanostructured PMMA Films**

doi:10.4028/0-00000-029-9.135